Mon. Not. R. Astron. Soc. **325,** 443–448 (2001)

Electron-impact rotational excitation of linear molecular ions

Alexandre Faure and Jonathan Tennyson★
Department of Physics and Astronomy, University College London, Gower Street, London WC1E 6BT

Accepted 2001 March 2. Received 2001 March 2; in original form 2001 February 16

ABSTRACT

Molecular R-matrix calculations are performed to give rotational excitation rates for electron collisions with linear molecular ions. Results are presented for CO^+, HCO^+, NO^+ and H_2^+ up to electron temperatures of 10 000 K. De-excitation rates and critical electron densities are also given. It is shown that the widely used Coulomb–Born approximation is valid for $\Delta j = 1$ transitions when the molecular ion has a dipole greater than about 2D, but otherwise is not reliable for studying electron-impact rotational excitation. In particular, transitions with $\Delta j > 1$ are found to have appreciable rates and are found to be entirely dominated by short-range effects.

Key words: molecular data – molecular processes – ISM: molecules.

1 INTRODUCTION

Since the discovery of CH^+ more than 50 years ago, several molecular ions have been observed in the interstellar medium (ISM). These, and other undetected ions, are known to play key roles in the gas-phase chemistry of interstellar clouds (Herbst 1995). Recent observations also suggest that the more reactive species might constitute specific tracers of harsh astronomical environments (Black 1998). CO^+, in particular, has been observed through several rotational transitions in various photodissociation regions (PDRs) (Latter, Walker and Maloney 1993), in the low-mass protostar IRAS 16293−2422 (Ceccarelli et al. 1998) and very recently towards the nucleus of Cygnus A (Fuente et al. 2000). HCO^+ is another astrophysically important species recently detected by a number of rotational transitions in star-forming regions (Rawlings, Taylor & Williams 2000), in the Orion Bar (Young Owl et al. 2000) and towards the star Cygnus OB2 No. 12 (Scappini et al. 2000). A good knowledge of the rotational excitation rates of such molecular ions is crucial for a critical interpretation of the observed spectra.

In diffuse environments, electrons are expected to be the most important exciting species for molecular ions. Cross-sections for electron-impact excitation are indeed several orders of magnitude greater than the corresponding ones for excitation by neutral species such as H and H_2. There are, however, no experimental determinations of electron-impact rotational excitation rates for molecular ions and, therefore, interstellar chemical models have relied exclusively on theoretical predictions. The reference method for studying electron-impact excitation of molecular ions is the Coulomb–Born approximation (Chu & Dalgarno 1974; Dickinson & Flower 1981; Neufeld & Dalgarno 1989). This theory assumes that the collisional excitation rates can be determined by long-range effects only. A standard further approximation is to consider only the dominant long-range term. Within this model, only single jumps in rotational quanta are allowed for polar ions. Recent R-matrix studies on HeH^+ (Rabadán, Sarpal & Tennyson 1998a) and CH^+ (Lim, Rabadán & Tennyson 1999) have suggested that the dipolar Coulomb–Born approximation is not a reliable method for computing rotational excitation rates. In particular, the R-matrix calculations have shown that electron collisions can change the rotational state by up to six quanta and that two quantum transitions can be comparable to or can be bigger than one quantum ones.

In this work, we present rotational electron-impact excitation rates for CO^+, HCO^+, NO^+ and H_2^+. Although they have not been detected in space, NO^+ and H_2^+ are thought to participate in the chemistry of harsh environments, NO^+ – vital component of the lower ionosphere of the Earth (Grebowsky & Bilitza 1999) – is an important species for the nitrogen chemistry occuring in PDRs (Young Owl et al. 2000) and H_2^+ – considered as a key species in the formation of H_2 in the early Universe (Rawlings, Drew & Barlow 1994) – might achieve high abundances in X-irradiated molecular gas (Black 1998). The aim of this work is to complete the previous R-matrix results (Rabadán et al. 1998a, Lim et al. 1999) on electron-impact rotational excitation rates for linear molecular ions, and to assess the importance of the short-range effects in various and representative systems. In Section 2, R-matrix calculations are described and the procedure used to obtain cross-sections is briefly introduced. In Section 3, we present and discuss our results. Conclusions are summarized in Section 4.

2 CALCULATIONS

2.1 R-matrix calculations

Electron–CO^+ collisions calculations were performed using the wavefunctions developed by Tennyson (1996a), where full details

★E-mail: j.tennyson@ucl.ac.uk

can be found. R-matrix calculations were performed at the CO equilibrium bond length of $R_e = 2.132\ a_0$, using an R-matrix sphere of radius 10 a_0. A fixed bond length is appropriate, as previous studies on HeH^+ and NO^+ have shown that rotational excitation cross-sections are rather insensitive to vibrational motion effects (Rabadán, Sarpal & Tennyson 1998b). The total wavefunctions were based on a close-coupling expansion, which include eight CO^+ states (the lowest three $^2\Sigma^+$ and $^2\Pi$ target states augmented by the lowest two states of $^2\Delta$ symmetry) generated by using a valence complete active space configuration interaction (CASCI) procedure. The close-coupling expansion was augmented by terms representing correlation and polarization. This model gives a ground state dipole moment of 2.516 D for CO^+, which is close to the best available theoretical value of 2.567 D (Martin & Fehér 1995). The continuum functions were generated as numerical solutions of an isotropic Coulomb potential with $l \leq 6$, $m \leq 2$ and energy below 136.06 eV. These calculations produced fixed-nuclei (FN) T-matrices for Σ^+, Π and Δ total symmetries, with both singlet and triplet states.

Electron-HCO^+ calculations were performed using the polyatomic UK R-matrix package (Tennyson & Morgan 1999). At the equilibrium geometry, HCO^+ is a linear molecule with $r(CH) = 2.074\ a_0$ and $R(CO) = 2.088\ a_0$ (Woods 1988). The HCO^+ molecular ion was represented using a double-zeta plus polarization (DZP) basis set (Dunning 1970). In the C_{2v} symmetry, this target basis consisted of 35 self-consistent field orbitals: $19a_1$, $7b_1$, $7b_2$ and $2a_2$. The two lowest target states of symmetry $^1\Sigma^+$ and $^3\Sigma^+$ were included in the close-coupling expansion. These states were generated using a valence CASCI procedure in which the 14 electrons of HCO^+ were distributed according to the prescription $1a_1^2 2a_1^2 (3a_1 4a_1 5a_1 6a_1 1b_1 2b_1 1b_2 2b_2)^{10}$. Polarization terms were also included. This model gives a ground state dipole moment of 4.064 D for HCO^+, which can be compared with the value of 3.9 D calculated by Yamaguchi, Richards & Schaefer (1994). The continuum orbitals were represented by Gaussian-type basis functions optimized to represent Coulomb functions (Faure et al. 2001), with $l \leq 4$ and energy below 68.03 eV. They consisted of $63a_1$, $41b_1$, $41b_2$ and $24a_2$ orbitals, which were Schmidt orthogonalized to the target orbitals (Tennyson & Morgan 1999). FN T-matrices, converted to the $C_{\infty v}$ symmetry, were obtained for total symmetries $^2\Sigma^+$, $^2\Pi$ and $^2\Delta$.

Electron–NO^+ collisions calculations were performed using the wavefunctions developed by Rabadán & Tennyson (1997), where full details can be found. R-matrix calculations were performed at the NO^+ equilibrium bond length of $R_e = 2.003\ a_0$, using an R-matrix radius of 15 a_0. The total wavefunctions were constructed using the 12 lowest NO^+ states, which were represented using a CASCI expansion. Correlation and orthogonality relaxing effects were also included. This model gives a ground-state dipole moment of 0.257 D for NO^+, which can be compared with the value of 0.310 D computed by Billingsley (1973). The continuum was represented using $l \leq 5 + m$, $m \leq 2$ numerical functions obtained in an isotropic Coulomb potential. FN T-matrices were obtained for total symmetries $^2\Sigma^+$, $^2\Pi$ and $^2\Delta$.

Electron–H_2^+ collisions calculations were performed using the wavefunctions developed by Tennyson (1996b), where full details can be found. R-matrix calculations were performed at the H_2^+ equilibrium bond length of $R_e = 2.0\ a_0$, using an R-matrix radius of 14 a_0. Three SCF orbitals were included for each of the σ_g, σ_u, π_u and π_g symmetries. This model gives a ground state quadrupole moment of 1.546 ea_0^2 for H_2^+, which can be compared with the best theoretical value of 1.639 ea_0^2 (Moss 1990). The continuum orbitals, with $l \leq 6$, were coupled with the three lowest target states $^2\Sigma_g^+$, $^2\Sigma_u^+$ and $^2\Pi_u$ for the required total symmetry. Polarization terms were also included. FN T-matrices were obtained for Σ^+, Π and Δ total symmetries, with both singlet and triplet states.

2.2 Rotational cross-sections

The rotational cross-sections were calculated following the recommended procedure of Rabadán et al. (1998b), as implemented in the program ROTIONS of Rabadán & Tennyson (1998). In this procedure, the FN T-matrices are frame-transformed from the body frame to the laboratory frame. Rotational cross-sections for low-l partial waves are then obtained. For transitions with $\Delta j \leq 2$, the Coulomb–Born approximation is evaluated to obtain the cross-section for the high-l waves not included in the FN T-matrices. The total cross-section is then calculated as the sum of the two contributions. For transitions with $\Delta j > 2$, the high-l contribution is negligible and the cross-section can be safely evaluated using FN T-matrices only. Finally, the known unphysical behaviour of cross-sections at rotational thresholds, common in adiabatic nuclei rotational (ANR) theories, is corrected using a simple kinematic ratio (Chandra & Temkin 1976).

For electron temperatures between 100 and 10 000 K, excitation rates are sensitive to collision energies in the range 0.001–10 eV. In practice, the cross-sections were calculated in the energy range $E_{min} = 0.01$ eV up to a maximum value of E_{max} ($\leq$10 eV), selected to avoid the threshold of the first electronically excited state of the molecular ions. Below E_{min} and above E_{max}, the contribution to the cross-sections was estimated using the same low-energy and high-energy extrapolation procedures as Rabadán et al. (1998a).

3 RESULTS AND DISCUSSION

The transition rates were obtained in the range 100–10 000 K assuming a Maxwellian velocity distribution for the electrons. For use in modelling, the temperature dependence of the transition rates, q, have been fitted using the form:

$$q(T) = a(T/300)^b \exp(-c/T), \tag{1}$$

where T is in Kelvin and q in $cm^3\ s^{-1}$. It should be noted that the kinematic correction used to force the cross-sections to zero at threshold leads to rate coefficients which do not obey detailed balance at low temperatures. De-excitation rates were therefore computed from the excitation ones using the detailed balance relation.

The critical electron density, n_{cr}, is defined as the density at which the collisional de-excitation rate is equal to the spontaneous radiative de-excitation rate:

$$n_{cr}(j, T) = \sum_{j'<j} \frac{A(j \rightarrow j')}{q(j \rightarrow j')}. \tag{2}$$

In practice for all systems considered here, it was assumed that the Einstein A coefficients for spontaneous emission were dominated by a single transition: $j \rightarrow j - 1$ for the dipolar systems and $j \rightarrow j - 2$ for H_2^+.

3.1 CO^+

Rate coefficients for rotational transitions in CO^+ starting from the rotational ground-state are presented in Fig. 1.

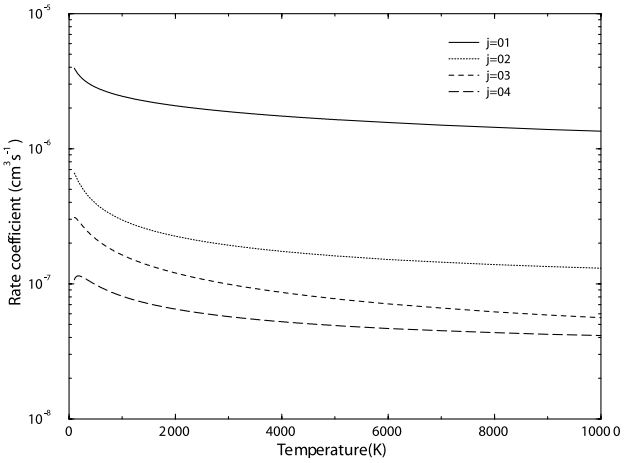

Figure 1. Rotational excitation rates for CO^+.

Table 1. Parameters fitted to the rate coefficients for CO^+. Rates were fitted to equation (1). Powers of 10 are given in parentheses.

Transition	a (cm^3 s^{-1})	b	c (K)
$j=0-1$	3.319(−6)	−0.2465	11.11
$j=0-2$	4.942(−7)	−0.4056	13.45
$j=0-3$	3.069(−7)	−0.4824	53.29
$j=0-4$	1.309(−7)	−0.3502	56.63
$j=1-0$	1.106(−6)	−0.2463	5.434
$j=1-2$	2.040(−6)	−0.2505	8.954
$j=1-3$	3.503(−7)	−0.3915	25.29
$j=1-4$	1.731(−7)	−0.4651	72.82
$j=2-0$	9.911(−8)	−0.4067	−2.551
$j=2-1$	1.224(−6)	−0.2504	−2.209
$j=2-3$	1.675(−6)	−0.2480	15.30
$j=2-4$	2.784(−7)	−0.3867	39.08
$j=3-0$	4.373(−8)	−0.4814	19.34
$j=3-1$	1.507(−7)	−0.3932	−1.490
$j=3-2$	1.197(−6)	−0.2481	−1.275
$j=3-4$	1.502(−6)	−0.2474	16.62
$j=4-0$	1.464(−8)	−0.3529	2.800
$j=4-1$	5.750(−8)	−0.4635	21.81
$j=4-2$	1.555(−7)	−0.3889	1.515
$j=4-3$	1.170(−6)	−0.2478	−5.354

It can be noticed that the excitation $j = 0 \rightarrow 1$ dominates all other processes. Significant rates are found, however, for higher transitions with Δj up to four. These higher transitions are ignored in a pure dipolar Coulomb–Born treatment. The fitted parameters of equation (1) are given in Table 1 for all important transitions. All fits reproduce our data within 2 per cent in the temperature range $100 \leq T \leq 5000$ K. At higher temperatures, the maximum discrepancy is less than 8 per cent.

For transitions with $\Delta j = 1$, the cross-sections were found to be dominated by long-range effects. This result is consistent with the large value of the CO^+ dipole moment (see Section 2.1), which leads to a very slow convergence of the dipolar Coulomb–Born cross-sections. In such a case, the low-partial waves contribution (calculated from FN T-matrices) is negligible. As a result, the Coulomb–Born approximation is sufficient to compute the $\Delta j = 1$ excitation rates. On the other hand, as previously noted by Rabadán et al. (1998b), transitions with $\Delta j > 1$ were found to be entirely dominated by low-partial waves. Moreover, as rotational excitation energies of CO^+ are very small (<0.005 eV for the above transitions), threshold effects were found to be significant at low temperatures only ($T < 300$ K). Critical densities for the various excitations are given in Table 2. These were computed using Einstein A coefficients calculated from the dipole moment using equation (3.1) of Dickinson & Flower (1981).

Table 2. Critical electron density, n_{cr} in cm^{-3}, as a function of temperature, for rotational levels in CO^+. Powers of 10 are given in parentheses.

T(K)	$j=1$	$j=2$	$j=3$	$j=4$
100	2.7(1)	2.0(2)	7.0(2)	1.7(3)
200	3.2(1)	2.5(2)	8.4(2)	2.0(3)
300	3.5(1)	2.7(2)	9.4(2)	2.3(3)
400	3.8(1)	3.0(2)	1.0(3)	2.5(3)
500	4.0(1)	3.2(2)	1.1(3)	2.7(3)
1000	4.7(1)	3.8(2)	1.3(3)	3.2(3)
2000	5.5(1)	4.5(2)	1.6(3)	3.9(3)
3000	6.1(1)	5.0(2)	1.8(3)	4.3(3)
4000	6.6(1)	5.4(2)	1.9(3)	4.7(3)
5000	7.0(1)	5.8(2)	2.0(3)	5.0(3)
6000	7.3(1)	6.1(2)	2.1(3)	5.2(3)
7000	7.7(1)	6.3(2)	2.2(3)	5.4(3)
8000	8.0(1)	6.6(2)	2.3(3)	5.6(3)
9000	8.2(1)	6.8(2)	2.4(3)	5.8(3)
10000	8.5(1)	7.0(2)	2.4(3)	6.0(3)

Table 3. Parameters fitted to the rate coefficients for HCO^+. Rates were fitted to equation (1). Powers of 10 are given in parentheses.

Transition	a (cm^3 s^{-1})	b	c (K)
$j=0-1$	9.169(−6)	−0.2479	12.83
$j=0-2$	1.317(−6)	−0.5198	22.84
$j=1-0$	3.055(−6)	−0.2478	8.413
$j=1-2$	5.384(−6)	−0.2421	9.756
$j=2-0$	2.633(−7)	−0.5196	9.842
$j=2-1$	3.229(−6)	−0.2420	1.031

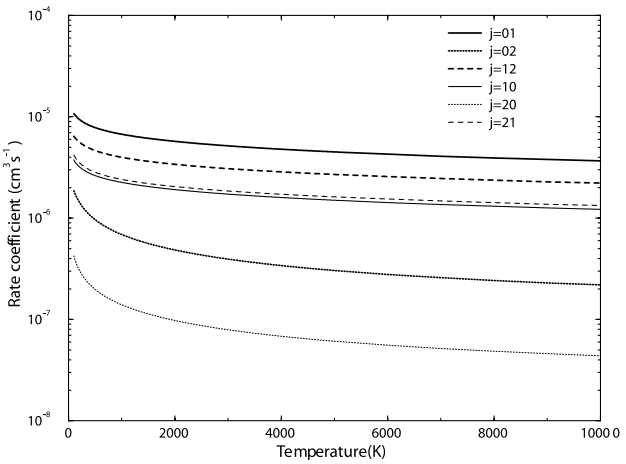

Figure 2. Rotational excitation and de-excitation rates for HCO^+.

3.2 HCO^+

Rate coefficients for rotational transitions with $\Delta j = 1$ and 2 in HCO^+ are presented in Fig. 2. Rates for higher transitions were found to be negligible. The fitted parameters of equation (1) are given in Table 3 for all important transitions. All fits agree to within

Table 4. Critical electron density, n_{cr} in cm^{-3}, as a function of temperature, for rotational levels in HCO^+. Powers of 10 are given in parentheses.

T(K)	$j = 1$	$j = 2$
100	1.2(1)	9.6(1)
200	1.4(1)	1.2(2)
300	1.6(1)	1.3(2)
400	1.7(1)	1.4(2)
500	1.8(1)	1.5(2)
1000	2.0(1)	1.7(2)
2000	2.4(1)	2.1(2)
3000	2.7(1)	2.3(2)
4000	2.9(1)	2.5(2)
5000	3.1(1)	2.6(2)
6000	3.2(1)	2.8(2)
7000	3.4(1)	2.9(2)
8000	3.5(1)	3.0(2)
9000	3.7(1)	3.1(2)
10000	3.8(1)	3.2(2)

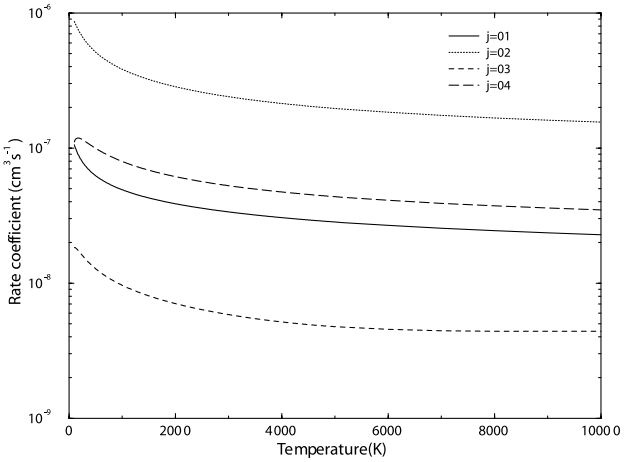

Figure 3. Rotational excitation rates for NO^+.

4 per cent with the calculated values for the entire temperature range.

As in CO^+, rotational cross-sections were found to be completely dominated by high-partial waves for transitions with $\Delta j = 1$, and by the low-partial waves contribution for those with $\Delta j = 2$. We also noticed that the bigger dipole moment of HCO^+ leads to $\Delta j = 1$ excitation rates significantly larger than the corresponding ones in CO^+. In fact, since the rotational constants of both species are very similar, the ratio between the CO^+ and HCO^+ $\Delta j = 1$ cross-sections is approximately equal to the ratio between the square of the respective dipoles [see equation (21) of Chu & Dalgarno 1974]. Critical electron densities were calculated using the same procedure as for CO^+. Tabulated values for excited rotational states are given in Table 4.

3.3 NO^+

Rate coefficients for rotational transitions in NO^+ starting from $j = 0$ are presented in Fig. 3. As NO^+ has a small dipole (see Section 2.1), short-range effects have a significant influence on $\Delta j = 1$ cross-sections. As a result, the Coulomb–Born calculation was found to underestimate $\Delta j = 1$ excitation rates by a factor of almost two. Another interesting and original feature of NO^+ is that

Table 5. Parameters fitted to the rate coefficients for NO^+. Rates were fitted to equation (1). Powers of 10 are given in parentheses.

Transition	a ($cm^3\ s^{-1}$)	b	c (K)
$j=0-1$	7.481(−8)	−0.3462	2.762
$j=0-2$	6.667(−7)	−0.4395	21.42
$j=0-3$	1.793(−8)	−0.4756	49.91
$j=0-4$	1.403(−7)	−0.4146	68.26
$j=1-0$	2.494(−8)	−0.3463	−2.943
$j=1-2$	5.453(−8)	−0.3659	7.216
$j=1-3$	4.562(−7)	−0.4315	33.49
$j=1-4$	9.942(−9)	−0.4597	69.09
$j=2-0$	1.335(−7)	−0.4402	4.522
$j=2-1$	3.274(−8)	−0.3662	−4.109
$j=2-3$	4.546(−8)	−0.3641	17.16
$j=2-4$	3.662(−7)	−0.4253	49.15
$j=3-0$	2.563(−9)	−0.4760	15.54
$j=3-1$	1.959(−7)	−0.4323	5.192
$j=3-2$	3.252(−8)	−0.3647	0.2427
$j=3-4$	4.184(−8)	−0.3647	22.16
$j=4-0$	1.563(−8)	−0.4156	11.32
$j=4-1$	3.319(−9)	−0.4603	17.62
$j=4-2$	2.039(−7)	−0.4263	9.434
$j=4-3$	3.260(−8)	−0.3655	−0.4032

Table 6. Critical electron density, n_{cr} in cm^{-3}, as a function of temperature, for rotational levels in NO^+. Powers of 10 are given in parentheses.

T(K)	$j = 1$	$j = 2$	$j = 3$	$j = 4$
100	7.6(1)	1.1(2)	2.8(2)	6.6(2)
200	9.8(1)	1.4(2)	3.7(2)	8.4(2)
300	1.1(2)	1.7(2)	4.3(2)	9.8(2)
400	1.3(2)	1.9(2)	4.9(2)	1.1(3)
500	1.4(2)	2.1(2)	5.4(2)	1.2(3)
1000	1.7(2)	2.8(2)	7.2(2)	1.6(3)
2000	2.2(2)	3.7(2)	9.7(2)	2.1(3)
3000	2.5(2)	4.4(2)	1.1(3)	2.5(3)
4000	2.8(2)	4.9(2)	1.3(3)	2.8(3)
5000	3.0(2)	5.4(2)	1.4(3)	3.1(3)
6000	3.2(2)	5.7(2)	1.5(3)	3.3(3)
7000	3.4(2)	6.0(2)	1.6(3)	3.4(3)
8000	3.5(2)	6.3(2)	1.6(3)	3.6(3)
9000	3.6(2)	6.5(2)	1.7(3)	3.7(3)
10000	3.7(2)	6.7(2)	1.7(3)	3.8(3)

$\Delta j = 2$ and $\Delta j = 4$ excitation rates are significantly larger than those with $\Delta j = 1$, which are assumed to be dominant in a pure dipolar Coulomb–Born treatment (Rabadan et al. 1998b). These results also illustrate the propensity rule for $\Delta j = 2$ transitions to dominate in quasi-homonuclear molecules.

The fitted parameters of equation (1) are given in Table 5 for all important transitions. All fits reproduce our data within 2 per cent in the temperature range $100 \leq T \leq 5000$ K. At higher temperatures, the maximum discrepancy is less than 8 per cent except for $\Delta j = 3$ transitions where it attains 25 per cent at 10 000 K. However, it should be noted that $\Delta j = 3$ excitation rates are very small. Critical electron densities, calculated as previously, are given in Table 6.

3.4 H_2^+

Rotational excitation cross-sections for the rotational transition $j = 0 \rightarrow 2$ in para-H_2^+ are presented in Fig. 4.

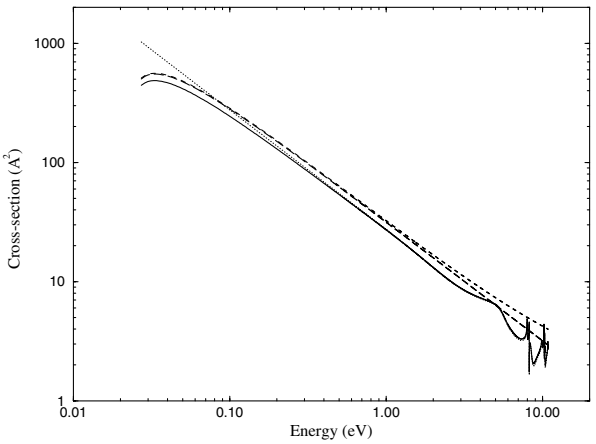

Figure 4. Rotational excitation cross-sections for the transition $j = 0 \rightarrow 2$ in para-H_2^+. Our results, with and without threshold correction, are represented by the solid and dotted lines, respectively. The dashed line gives the Coulomb–Born approximation. The long-dashed line gives the results of Stabler (1963), based on a low-energy expansion of the Coulomb–Born approximation.

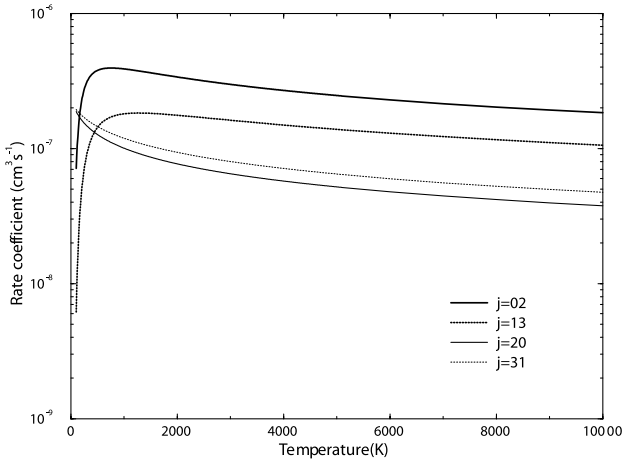

Figure 5. Rotational excitation and de-excitation rates for ortho and para H_2^+.

Table 7. Parameters fitted to the rate coefficients for ortho and para H_2^+. Rates were fitted to equation (1). Powers of 10 are given in parentheses.

Transition	a ($cm^3 s^{-1}$)	b	c (K)
$j = 0–2$	8.943(−7)	−0.4323	314.8
$j = 2–0$	1.699(−7)	−0.4116	39.21
$j = 1–3$	5.036(−7)	−0.4194	516.7
$j = 3–1$	1.956(−7)	−0.3816	48.09

It should be noted that the apparent agreement between our results and the Coulomb–Born approximation is accidental since $\Delta j = 2$ cross-sections are completely dominated by the low-partial waves, as already suggested by Dickinson & Muñoz (1977). It can also be noticed that the threshold correction is important at energies lower than about 0.1 eV, which means that threshold effects are significant for relatively high temperatures ($T < 2000$ K). Rate coefficients are shown in Fig. 5.

Table 8. Critical electron density, n_{cr} in cm^{-3}, as a function of temperature, for rotational levels in ortho and para H_2^+. Powers of 10 are given in parentheses.

T(K)	$j = 2$	$j = 3$
100	5.3(−5)	8.2(−4)
200	6.1(−5)	9.1(−4)
300	6.7(−5)	9.8(−4)
400	7.3(−5)	1.0(−3)
500	7.8(−5)	1.1(−3)
1000	9.9(−5)	1.3(−3)
2000	1.3(−4)	1.7(−3)
3000	1.5(−4)	2.0(−3)
4000	1.7(−4)	2.3(−3)
5000	1.9(−4)	2.5(−3)
6000	2.1(−4)	2.7(−3)
7000	2.2(−4)	2.9(−3)
8000	2.4(−4)	3.1(−3)
9000	2.5(−4)	3.2(−3)
10000	2.6(−4)	3.4(−3)

Transitions with $\Delta j = 4$ were found to be negligible. The fitted parameters of equation (1) are given in Table 7 for the relevant transitions. Fits agree to within 4 per cent with the calculated values for the whole temperature range.

Critical electron densities are given in Table 8. The Einstein A coefficients were calculated from the quadrupole moment using the formulae given in Posen, Dalgarno & Peek (1983). Our values agree within 2 per cent with those of Posen et al. (1983). It should be noted that the long lifetime of the excited rotational states of H_2^+ leads to very low values for the critical density.

4 CONCLUSIONS

The electron-impact rotational excitation rates presented here for the linear molecular ions CO^+, HCO^+, NO^+ and H_2^+ should be considered along with the similar rates for HeH^+ (Rabadán et al. 1998a) and CH^+ (Lim et al. 1999). Previous studies found that the dipole Coulomb–Born approximation was poor for all transitions even when an allowance was made for near-threshold effects, which was found necessary for light systems such as HeH^+ and CH^+. Conversely we found that the dominant $\Delta j = 1$ transitions for CO^+ and, especially, HCO^+ were well represented by the Coulomb–Born approximation. The distinction is that CO^+ and HCO^+ have very large-permanent dipole moments, in excess of 2 D. In fact HeH^+ also has a large-permanent dipole (1.7 D), but this is insufficient to totally dominate the electron-impact rotational excitation rate. It would therefore appear that the Coulomb–Born approximation is reliable for $\Delta j = 1$ transitions in cases where the molecular ion has a dipole in excess of about 2D.

Conversely, our study and the previous ones have found all results for $\Delta j > 1$ transitions to be dominated by short-range interactions. We do find in all cases that at least $\Delta j = 2$ transitions are significant, and in some cases higher transitions as well. This result is important. In environments below the critical density, it has often been assumed that molecular ions rotationally excited by electron impacts will emit $j = 1 \rightarrow 0$ photons only. Our calculations suggest that in all cases considered so far a significant flux of $j = 2 \rightarrow 1$ should also be emitted and in some cases, particularly NO^+, emissions from higher rotational states should also be important.

Of course not all astronomically important molecular ions are linear. We are at present extending the theory of Rabadán et al. (1998b) to consider non-linear molecules, focusing on the important, triangular H_3^+ ion.

ACKNOWLEDGMENTS

We thank Ismanuel Rabadán for providing the NO^+ wavefunctions. Part of the calculations were carried out on the workstations of the 'Service Commun de Calcul Intensif de l'Observatoire de Grenoble' with the valuable help of Pierre Valiron. AF grateful acknowledges the European Union for the provision of a Marie Curie Fellowship number HPMF-CT-1999-00415.

REFERENCES

Billingsley F. P., 1973, Chem. Phys. Lett., 23, 160
Black J., 1998, Faraday. Discuss., 109, 257
Ceccarelli C., Caux E., Wolfire M., Rudolph A., Nisini B., Saraceno P., White G. J., 1998, A&A, 331, L17
Chandra M., Temkin A., 1976, Phys. Rev. A, 13, 88
Chu S.-I., Dalgarno A., 1974, Phys. Rev. A, 10, 788
Dickinson A. S., Flower D. R., 1981, MNRAS, 196, 297
Dickinson A. S., Muñoz J. M., 1977, J. Phys. B: At. Mol. Opt. Phys., 10, 3151
Dunning T. H., 1970, J. Chem. Phys, 53, 2823
Faure A., Gorfinkiel J., Morgan L., Tennyson J., 2001, Computer. Phys. Commun., submitted
Fuente A., Black J. H., Martín-Pintado J., Rogríguez-Franco A., García-Burillo S., Planesas P., Lindholm J., 2000, ApJ, 545, L113
Grebowsky J. M., Bilitza D., 1999, Adv. Space Res., 25, 183
Herbst E., 1995, Annu. Rev. Phys. Chem., 46, 27
Latter W. B., Walker C. K., Maloney P. R., 1993, ApJ, 419, L97
Lim A., Rabadán I., Tennyson J., 1999, MNRAS, 306, 473
Martin P. A., Fehér M., 1995, Chem. Phys. Lett., 232, 491
Moss R. E., 1990, Chem. Phys. Lett., 172, 6
Neufeld D. A., Dalgarno A., 1989, Phys. Rev. A., 40, 633
Posen A. G., Dalgarno A., Peek J. M., 1983, At. Data Nucl. Data Tables, 28, 265
Rabadán I., Tennyson J., 1997, J. Phys. B: At. Mol. Opt. Phys., 30, 1975
Rabadán I., Tennyson J., 1998, Computer Phys. Commun., 114, 129
Rabadán I., Sarpal B. K., Tennyson J., 1998a, MNRAS, 299, 171
Rabadán I., Sarpal B. K., Tennyson J., 1998b, J. Phys. B: At. Mol. Opt. Phys., 31, 2077
Rawlings J. M. C., Drew J. E., Barlow M. J., 1994, MNRAS, 265, 968
Rawlings J. M. C., Taylor S. D., Williams D. A., 2000, MNRAS, 313, 461
Scappini F., Cecchi-Pestellini C., Codella C., Dalgarno A., 2000, MNRAS, 317, L6
Stabler R. C., 1963, Phys. Rev., 131, 679
Tennyson J., 1996a, J. Phys. B: At. Mol. Phys., 29, 6185
Tennyson J., 1996b, At. Data Nucl. Data Tables, 64, 253
Tennyson J., Morgan L., 1999, Phil. Trans. R. Soc. Lond. A, 357, 1161
Woods R. C., 1988, Phil. Trans. R. Soc. Lond. A, 324, 141
Yamaguchi Y., Richards C. A., Jr., Schaefer H. F., 1994, J. Chem. Phys, 101, 8945
Young Owl R. C., Meixner M. M., Wolfire M., Tielens A. G. G. M., Tauber J., 2000, ApJ, 540, 886

This paper has been typeset from a TEX/LATEX file prepared by the author.